IEEE Photonics Journal
An IEEE Photonics Society Publication

Open Access

A Widely Tunable Directly Modulated DBR Laser With High Linearity

Volume 6, Number 4, August 2014

Liqiang Yu
Huitao Wang
Dan Lu
Song Liang
Can Zhang
Biwei Pan
Limeng Zhang
Lingjuan Zhao

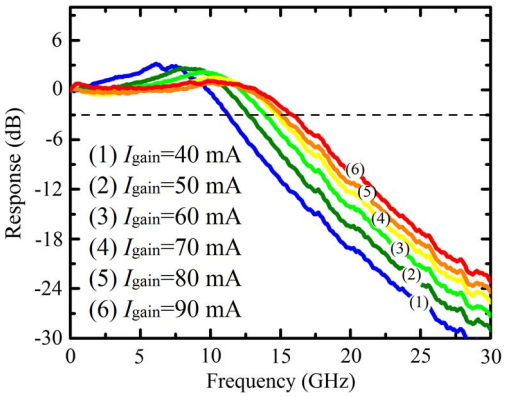

DOI: 10.1109/JPHOT.2014.2331247
1943-0655 © 2014 IEEE

A Widely Tunable Directly Modulated DBR Laser With High Linearity

Liqiang Yu, Huitao Wang, Dan Lu, Song Liang, Can Zhang, Biwei Pan, Limeng Zhang, and Lingjuan Zhao

Key Laboratory of Semiconductor Materials Science, Institute of Semiconductors, Chinese Academy of Science, Beijing 100086, China

DOI: 10.1109/JPHOT.2014.2331247

Manuscript received May 19, 2014; revised June 11, 2014; accepted June 12, 2014. Date of publication June 18, 2014; date of current version July 9, 2014. This work was supported in part by the National 973 Program under Grant 2011CB301702, by the National 863 Project under Grant 2013AA014202, and by the National Natural Science Foundation of China under Grants 61201103, 61335009, 61274045, and 61205031. Corresponding author: L. Yu (e-mail: yuliqiang10@semi.ac.cn).

Abstract: We demonstrate a widely tunable and high-modulation-bandwidth distributed Bragg reflector (DBR) laser. With the selected butt-joint material ($\lambda g = 1.44\ \mu m$) and butt-joint angle (45°) for the grating section, a widely tuning range of 13.88 nm with 19 consecutive channels is obtained for the two-section DBR laser. Furthermore, a small-signal modulation bandwidth of 16 GHz with in-band flatness of ± 3 dB is realized at 10 °C. A uniform modulation bandwidth of more than 13 GHz is obtained for ten consecutive channels at 25 °C. Meanwhile, the DBR laser shows a high linearity, with an input 1-dB compression point of 17 dBm and an input third-order intercept point of 30 dBm at 13 GHz.

Index Terms: Directly-modulated, Distributed Bragg reflector (DBR) lasers, Passive optical networks (PONs).

1. Introduction

Passive optical networks (PONs) have been widely considered as the ultimate solution for future access networks. At the April 2012 meeting of the Full Service Access Network (FSAN) community, time and wavelength division multiplexed passive optical network (TWDM-PON) has been selected as the primary broadband solution after 10G PONs [1]. As a chosen solution for next-generation passive optical network stage-2 (NG-PON2) architecture, the TWDM-PON can reuse the mature 10G PONs technology and other commercial components. Yet, the system configuration still faces unique technique challenges, among which the cost-effective colorless laser source is an indispensable technology [2]. Very recently, Huawei has developed the world's first optical transceivers for 40 Gbps TWDM-PONs [3]. In the proposed system, a three-section DBR laser with external modulation is used as the tunable transmitter for 10 Gb/s upstream transmission, while four 10 Gb/s EMLs (electro-absorption modulated lasers) with different wavelengths are used for the downstream. However, all those external modulators usually introduce losses to the transmitted power due to their coupling and insertion losses. Usually, an additional semiconductor optical amplifier is integrated to compensate for the insertion loss of the modulator. Those aspects would lead to increased complexity and cost of the transmitter. Therefore, direct modulation laser (DML) seems to be a convenient way only to meet the twin constraints of low-cost and high performance for the access network [4].

For transmitters used in optical network unit (ONU), they should be compact, low-cost, and have a wavelength tuning range sufficient for the TWDM-PON [5]. Thanks to the widely tuning range and fast tuning speed, compared with the thermal tuning of the distributed feedback (DFB) lasers, the monolithic tunable distributed Bragg reflector (DBR) lasers are good candidates for the colorless laser sources in digital optical communication systems. Besides, wavelength-tunable directly modulated DBR lasers with high linearity can also find their applications in analog signal transmission links, which are widely used in cable TV (CATV) systems [6], radar systems, and radio over fiber (RoF) systems [7].

Yet, previous investigations on the direct modulation of DBR lasers mainly focused on the sampled-grating distributed Bragg reflector (SGDBR) lasers, due to their large tuning ranges ($>$ 40 nm) and thus being promising candidates in dense wave-length-division multiplexing (DWDM) systems [8]. As we know, the results reported on the direct modulation bandwidth of SGDBR lasers are not sufficient. For example, Lee *et al.* realized a modulation bandwidth of 4 GHz [9], and carried out the transmission experiments of only 1.244 Gb/s [10]. By improving the differential quantum efficiency, Klamkin *et al.* has reported an improved direct modulation performance, in which, however, the bandwidth is not larger than 5 GHz [11]. Compared to the SGDBR lasers with two sampled reflectors, a two-section DBR laser (a gain section and a DBR section) possibly can realize a higher-speed direct modulation, due to the shortened cavity length [2]. Besides, the simple structure with one reflector enables a reduced cost in all those processes including fabrication, packaging, and usage, which will greatly benefit the ONU systems.

Prior to this, our fabricated DBR laser has successfully realized a 40 km single-mode fiber transmission with 2.5 Gb/s modulation rate [12]. The results indicate that it is a good candidate for 40G G-PON ONU transmitter. However, the modulation rate is small, and also the wavelength tuning range. Larger tuning range can be obtained by changing the working temperature which inevitably influences the output power. Here, in this paper, we present a two-section DBR laser which has a wider tuning range and a larger modulation bandwidth. By using an InGaAsP quaternary with band gap of 1.44 μm (λg = 1.44 μm) as the butt-joint material of the Bragg grating, a wavelength tuning range of 13.88 nm is obtained. A 16-GHz 3-dB modulation bandwidth is obtained for 10 °C. Meanwhile, a uniform bandwidth of larger than 13 GHz is obtained for a consecutive 10-channel at 25 °C. Besides digital optical communication systems, potential use of the DBR laser in analog systems is also investigated by measuring the input 1-dB compression point and input third-order intercept point.

2. Device Design and Fabrication

The study here mainly focuses on what material and design parameters affecting the wavelength tuning and how to increase the tuning range. The first parameter in question is the composition of the material which forms the Bragg grating of the tunable lasers (TLs). Different grating material strongly affects the effective index change [13], which in turn influences the tuning range. It is shown that there is an obvious advantage at butt-jointing grating materials with a bandgap wavelength closer to the lasing wavelength, where we can obtain a larger index change and thus a larger tuning range. By using an InGaAsP quaternary of 1.42-μm bandgap (λg = 1.42 μm) as the grating material, a maximum tuning range of 15 nm is numerically estimated [14], while in [15], a 1.3Q grating material just generates a 4.4-nm continuous tuning range. Nevertheless, the bandgap of the butt-joint material should be not so large that the absorption losses increase greatly. Here we use a 1.44Q InGaAsP quaternary (λg = 1.44 μm) as the butt-joint material, as shown in Fig. 1. The photoluminescence (PL) peak of the gain section is around 1530 nm. The 90-nm wavelength detuning can enable a sufficiently low absorption loss. At the beginning of the tuning, the Bragg wavelength (λ_B) is selected to about 1540 nm, marked by the dashed arrow in Fig. 1. It is noted that the mutual positions of the gain spectra and the Bragg reflectivity spectra also affect the tuning performance and the best tuning performance can be achieved when the Bragg wavelength is red-shift with respect to the PL peak of

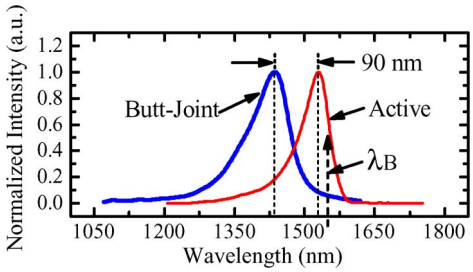

Fig. 1. Photoluminescence (PL) spectra of the active material and the butt-joint material. The Bragg wavelength before tuning is marked by the black dash line.

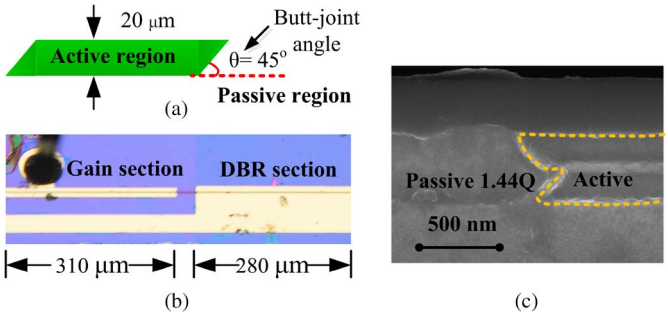

Fig. 2. (a) Schematic diagram of illustrating the butt-joint angle. Here, the schematic diagram is the top view of the photolithography mask for the butt-joint process. (b) Photograph of the tunable laser. (c) SEM image of the butt-joint cross-sectional profile.

the gain section [14]. Nevertheless, a negative detuning between the Bragg wavelength and the PL peak can result in higher differential gain, and then increase the modulation bandwidth. So, we make a compromise between maintaining the modulation bandwidth and increasing the tuning range by selecting a positive detuning of around 10 nm at the beginning of the tuning.

For the DBR lasers here based on a butt-joint technique, another critical factor that influences the tuning performance is the butt-joint angle between the gain section and the DBR section [16]. A large reflection derived from the butt-joint interface may result an irregular wavelength shifting with the DBR current. Therefore, the angle should be optimized to obtain a small reflectivity while maintaining a good transmission between the gain section and the DBR section to realize a high output power. We design our lasers with a butt-joint angle of 45, which is a good trade-off between reduced reflectivity and acceptable transmission. Fig. 2(a) shows the top view of the photolithography mask for the butt-joint process, where the width of the active region is 20 μm, and the angle between the active region and passive region is 45°. Besides, a typical SEM image of the butt-joint cross-sectional profile is shown in Fig. 2(c).

The photograph of the fabricated DBR laser is shown in Fig. 2(b). The device structure is grown by three-step metal organic chemical vapor deposition (MOCVD) on *n*-InP substrates. This structure has a symmetrical cladding and the active region is composed of 6 undoped InGaAsP quantum wells with a 1.53 μm PL peak. After a first epitaxy, the MQW and cladding layers in the DBR section is removed, and then a 300-nm thick InGaAsP layer ($\lambda g = 1.44$ μm) is filled with a butt-joint angle of 45°. After that, a grating was formed in the butt-joint waveguide layer of the DBR section through holographic lithography and dry etching. The final growth of *p*-doped top cladding was done still by MOCVD. A 3 μm ridge-waveguide is formed to minimize the thermal saturation while preserving lateral single-mode operation. A 50-μm isolation section between the gain section and DBR section are accomplished by etching the *p*-InGaAs layer off and He+ implantation. A Ti-Au metal layer is sputtered on the *p*-InGaAs contact layer to form a p-contact. After the substrate is thinned, Au-Ge-Ni metal is evaporated on the backside. Finally,

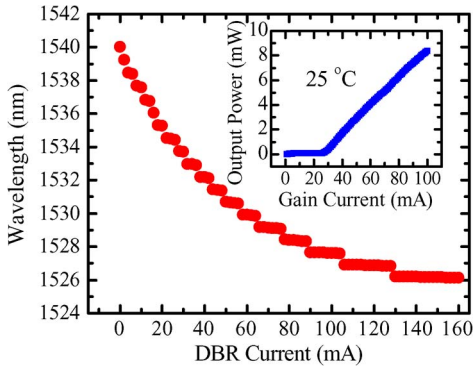

Fig. 3. Measured wavelength tuning as a function of the DBR current at 25 °C. The inset shows the output power versus the gain current at 25 °C.

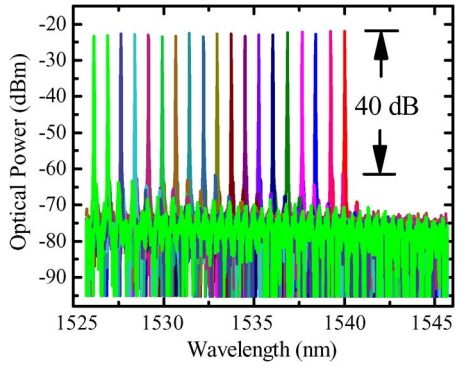

Fig. 4. Measured overlapped spectra of a 19-channel consecutive wavelength when only tuning the DBR current.

chips composed of a 310-μm gain section and a 280-μm DBR section are cleaved with both sides uncoated. The cavity length can enable us to obtain a mode-spacing of around 0.8 nm. The laser from the uncoated facet of the gain section is coupled out using a tapered single mode fiber.

3. Results and Discussion

We first investigate the wavelength tuning range by changing the DBR section current. Fig. 3 shows the wavelength of the main mode as a function of the DBR current. In this example, the gain current is fixed at 90 mA and the working temperature is kept at 25 °C. As can be seen, when the DBR current increases from 0 mA to 160 mA, the lasing wavelength switches digitally over 19 consecutive channels. With an around 0.77-nm channel spacing, the tuning range of 13.88 nm is realized. As the current increases, the channel wavelength decreases, which indicates the tuning is dominated by the carrier injection effect rather than thermal effect. But when the DBR current is larger than 160 mA, a tuning saturation occurs due to the predominating thermal effect. In addition to the tuning range, the stability of the output power during tuning is also very important. Normally, biasing the DBR section will induce loss (free carrier absorption), which will reduce the lasing power. When the DBR current is 0 mA, the output power is 8.5 mW for 100-mA gain current, as shown in the inset of Fig. 3. An output power change of around 1.4 dB is obtained during the wavelength tuning. Plotted in Fig. 4 are the overlapped spectra of a 19-channel consecutive wavelength switching. Here, we change the coupling efficiency of the fiber in order to obtain an equivalent fiber-coupled power for each wavelength. The side mode suppression ratios (SMSRs) of larger than 40 dB are obtained for all channels. Besides, the

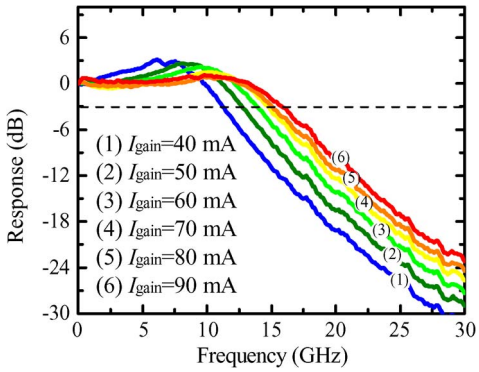

Fig. 5. Measured small-signal modulation response of the DBR laser for different gain currents at 10 °C.

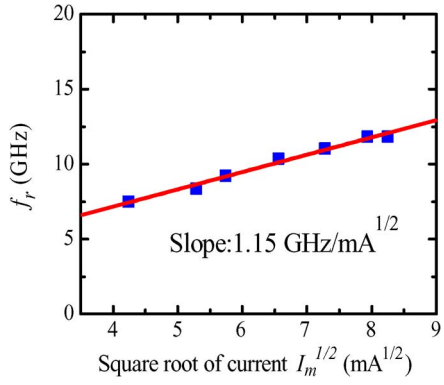

Fig. 6. Measured relaxation oscillation frequency of the DBR laser at 10 °C. Here, $I_m^{1/2} = (I_{gain} - I_{th})^{1/2}$.

far-field pattern (FFP) of the laser is measured with a value of 26° × 40° (horizontal × vertical), when the gain and DBR currents are 90 and 0 mA, respectively.

In order to evaluate the dynamic performance of the device, the modulation responses are carried out. Using a HP 8510C Network Analyzer, a small signal modulation response of the DBR laser is measured, as shown in Fig. 5, where the working temperature is fixed at 10 °C. As the gain current increases from 40 mA to 90 mA and the DBR current is fixed at 0 mA, the 3-dB modulation bandwidth increases from 11 GHz to 16 GHz. Besides, over-shoots in the resonance peak reducing from 3 dB to 1 dB are measured when increasing the gain current. As being important to determine the property of directly modulated operation, the relaxation oscillation frequency f_r is measured. Plotted in Fig. 6 is the measured f_r as a function of $(I_{gain} - I_{th})^{1/2}$, in which a maximum f_r of 11.8 GHz and a slope value of 1.15 GHz/mA$^{1/2}$ are obtained. Here, the DBR current is also fixed at 0 mA. A shorter cavity length can be used to increase the relaxation oscillation frequency, and hence increase the modulation bandwidth.

The dependence of the small signal modulation response on the temperature is also investigated. Fig. 7 shows the small signal modulation response at 10 °C, 25 °C, and 40 °C, respectively. When the temperature increases, the modulation bandwidth decreases together with an increased over-shoot. As shown in Fig. 8, we also extracted 3-dB bandwidths from the measured small signal responses and plotted them versus the square root of the current increment from the threshold current $(I_m^{1/2} = (I_{gain} - I_{th})^{1/2})$. It is well known that the 3-dB bandwidth is proportional to $I_m^{1/2}$ [17], [18], and we obtain a proportional constant of 12.3 GHz/mA$^{0.5}$ at 10 °C. The 3-dB bandwidth saturation will occur for large gain current due to a damping effect [18].

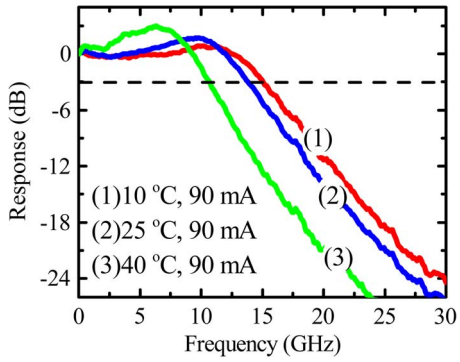

Fig. 7. Measured small-signal modulation response at different temperatures.

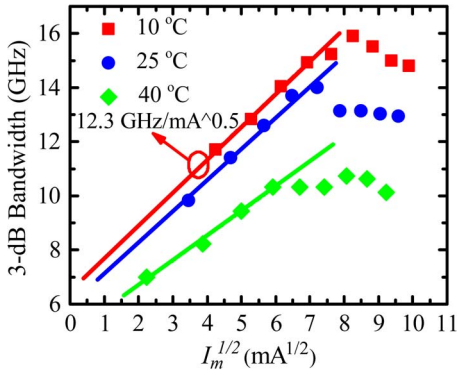

Fig. 8. Measured 3-dB direct modulation bandwidth versus gain currents at different temperatures. Here, $I_m^{1/2} = (I_{gain} - I_{th})^{1/2}$.

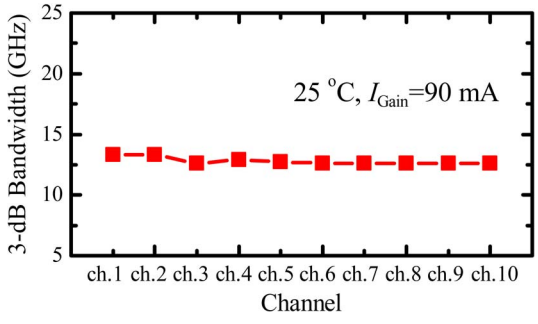

Fig. 9. Measured 3-dB direct modulation bandwidth for a 10-channel at 25 °C.

When the temperature increases, a small gain current may result in the bandwidth saturation. For example, at 10 °C, the saturation occurs when the gain current is 100 mA, while at 40 °C, an 80-mA gain current will result in the saturation. Here, the thresholds of the laser at 10 °C and 40 °C are around 22 and 34 mA, respectively. Therefore, by using an InGaAlAs MQW material to improve the temperature characteristic, the modulation bandwidth can be further improved.

As a widely tunable transmitter used in PONs systems, a uniform modulation bandwidth for all channels is crucial. Fig. 9 shows the 3-dB modulation bandwidth of a 10-wavelength-channel, when the gain current is fixed at 90 mA and the temperature is 25 °C. In this example, the wavelength of channel 1 is 1540 nm, and the spacing between each channel is around 0.8 nm. For

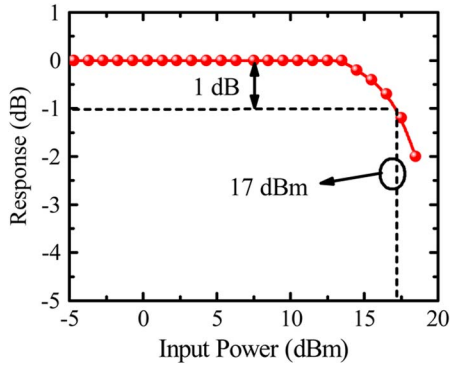

Fig. 10. Measured input 1-dB compression point of the laser operated at 13 GHz.

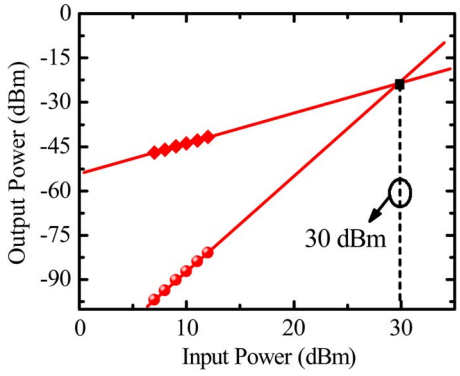

Fig. 11. Measured third-order intercept point of the laser operated at 13 GHz.

the 10 channels, a uniform bandwidth of higher than 13 GHz is obtained, which is valuable for a widely tunable transmitter operated in direct modulation.

For analog communication application, a straightforward limitation for the linearity of directly modulation is the 1 dB compression point. It means that the output light is 1-dB less than what would be obtained through a linear response. As shown in Fig. 10, the response of the laser remains constant in a wide power range. An input 1 dB compression point of 17 dBm is obtained at 13 GHz for channel 1. If the noise level of receiver is lower than -70 dBm, a dynamic range of 87 dB will be obtained.

For the directly modulated laser, we also measure the third-order intercept point. Due to the nonlinearity of the laser, distort and intermodulation signals will be contained in the output signal [19]. When two signals $f_0 + f$ and $f_0 - f$ are injected into the laser with the same energy, the third-order products $f_0 + 3f$ and $f_0 - 3f$ may be generated. Fig. 11 shows the output power of the fundamental and third-order intermodulation products versus the input power at 13 GHz. With f of 30 MHz, an input third-order intercept point of 30 dBm is obtained. This value is in excess of that measured by DFB lasers operating up to 10 GHz [20]. The results mean that the DBR laser is also qualified as transmitter in analog communication system.

4. Conclusion

We have fabricated and demonstrated a widely tunable DBR laser which has a modulation bandwidth as high as 16 GHz at 10 °C. Thanks to the selected butt-joint grating material ($\lambda g = 1.44\ \mu m$) and butt-joint angle (45°), a widely tuning range of 13.88 nm with a consecutive 19-channel is obtained. Besides, due to the high relaxation oscillation frequency, the maximum modulation bandwidth of 14 GHz is obtained for 25 °C and 16 GHz for 10 °C. In addition, a

uniform bandwidth of larger than 13 GHz is realized for a 10-channel wavelength. The results indicate that this compact and low-cost laser is a promising candidate as a colorless light source in TWDM-PON systems. An input 1-dB compression point of 17 dBm and a good intermodulation distortion with input third-order intercept of 30 dBm are measured at 13 GHz, which further shows its potential application for the analog optical communication systems.

Acknowledgment

The authors wish to thank Mingchao Chang for his careful assistance in measurements.

References

[1] FSAN next generation PON task group, [Online]. Available: http://www.fsan.org/task-groups/ngpon/
[2] B. Choi *et al.*, "10-Gb/s direct modulation of polymer-based tunable external cavity lasers," *Opt. Exp.*, vol. 20, no. 18, pp. 20368–20375, Aug. 2012.
[3] N. Cheng *et al.*, "World's first demonstration of pluggable optical transceiver modules for flexible TWDM PONs," presented at the 39th ECOC, 2013, vol. 1, pp. 1269–1271.
[4] J. Kreissl *et al.*, "Up to 40 Gb/s directly modulated laser operating at low driving current: Buried-heterostructure passive feedback laser (BH-PFL)," *IEEE Photon. Technol. Lett.*, vol. 24, no. 5, pp. 362–364, Mar. 2012.
[5] N. Cheng *et al.*, "Flexible TWDM PON system with pluggable optical transceiver modules," *Opt. Exp.*, vol. 22, no. 2, pp. 2078–2091, Jan. 2014.
[6] S. Itakura *et al.*, "High-current backside-illuminated photodiode array module for optical analog links," *J. Lightw. Technol.*, vol. 28, no. 6, pp. 965–971, Mar. 2010.
[7] D. Wake *et al.*, "A comparison of radio over fiber link types for the support of wideband radio channels," *J. Lightw. Technol.*, vol. 28, no. 16, pp. 2416–2422, Aug. 2010.
[8] S. Lee, F. Jang, and C. Wang, "Monolithically integrated multiwavelength sampled grating DBR lasers for dense WDM applications," *IEEE J. Sel. Topics Quantum Electron.*, vol. 6, no. 1, pp. 197–206, Jan. 2000.
[9] B. Mason, M. E. Heimbuch, and L. A. Coldren, "Directly modulated sampled grating DBR lasers for long-haul WDM communication systems," *IEEE Photon. Technol. Lett.*, vol. 9, no. 3, pp. 377–379, Mar. 1997.
[10] D. A. Tauber, V. Jayaraman, M. E. Heimbuch, L. A. Coldren, and J. E. Bowers, "Dynamic responses of widely tunable sampled grating DBR lasers," *IEEE Photon. Technol. Lett.*, vol. 8, no. 12, pp. 1597–1599, Dec. 1996.
[11] J. Klamkin *et al.*, "High efficiency widely tunable SGDBR lasers for improved direct modulation performance," *IEEE J. Sel. Topics Quantum Electron.*, vol. 11, no. 5, pp. 931–938, Sep. 2005.
[12] X. Yan *et al.*, "Tunable laser for 40GPON ONU transmitter," presented at the Nat. Fiber Optic Eng. Conf., 2012, pp. 1–3, NTu1J.5.
[13] J.-P. Weber, "Optimization of the carrier-induced effective index change in InGaAsP waveguides-application to tunable Bragg filters," *IEEE J. Quantum Electron.*, vol. 30, no. 8, pp. 1801–1816, Aug. 1994.
[14] G. Kyritsis and N. Zakhleniuk, "Self-consistent simulation model and enhancement of wavelength tuning of InGaAsP/InP multisection DBR laser diodes," *IEEE J. Sel. Top. Quantum Electron.*, vol. 19, no. 5, pp. 1–11, Sep. 2013.
[15] S. Murata, I. Mito, and K. Kobayashi, "Tuning ranges for 1.5 μm wavelength tunable DBR lasers," *Electron. Lett.*, vol. 24, no. 10, pp. 577–579, May 1988.
[16] Y. Zhang, "Design of ultra-high power multisection tunable lasers," *IEEE J. Sel. Top. Quantum Electron.*, vol. 12, no. 4, pp. 760–766, Jul. 2006.
[17] O. K. Kwon *et al.*, "A 10 $\times$ 10 Gb/s DFB laser diode array fabricated using a SAG technique," *Opt. Exp.*, vol. 22, no. 8, pp. 9073–9080, Apr. 2014.
[18] K. Takeda, T. Sato, A. Shinya, K. Nozaki, and W. Kobayashi, "Few-fJ/bit data transmissions using directly modulated lambda-scale embedded active region photonic-crystal lasers," *Nat. Photon.*, vol. 7, pp. 569–575, Jul. 2013.
[19] R. J. Ram and R. Helkey, "Linearity and third-order intermodulation distortion in DFB semiconductor lasers," *IEEE J. Quantum Electron.*, vol. 35, no. 8, pp. 1231–1237, Aug. 1999.
[20] P. Hartmann *et al.*, "Demonstration of highly linear uncooled DFB lasers for next generation RF over fibre applications," presented at the 28th Euro. Conf. Opt. Commun., Copenhagen, Denmark, pp. 1–2, 2002.